

# Analysis of the performance of GEM chambers for the upgrade of the LHCb muon system



## Public Note

Issue: 1  
Revision: 0

Reference: LHCb-14-2015  
Created: March 5, 2014  
Last modified: September 16, 2021

Prepared by: D. Pinci<sup>1</sup> and M. Santimaria<sup>2</sup>

<sup>1</sup>INFN - Sezione di Roma, Italy

<sup>2</sup>Università di Roma La Sapienza, Italy



## Abstract

Triple-GEM chambers, so far used in the inner region of the M1 muon station, are the ideal candidates to replace the MWPCs in the regions where, after the upgrade, the particle rate will be as high as  $2 \text{ MHz/cm}^2$ . Testing the triple-GEM efficiency and time resolution with different gaseous mixtures is therefore a significant step in evaluating the expected performance of the muon system after the upgrade scheduled in 2018, when the luminosity at LHCb will reach  $2 \times 10^{33} \text{ cm}^{-2}\text{s}^{-1}$ .

In this note, the study of the GEM efficiency and time performance is presented. Two gas mixtures are used for the measurements: Ar/CO<sub>2</sub>/CF<sub>4</sub> 40:55:5 and 45:15:40. A preliminary simulation of the gas mixtures properties is performed using the software GARFIELD, focusing on electron drift velocity and specific ionization. Several measurements of efficiency and time performance of the triple-GEM were then made by means of cosmic rays by changing the detector electric fields and the voltages across the GEM foils. The experimental results agree with the computed simulation: with the 5 % CF<sub>4</sub> gas mixture a detection efficiency in a 25 ns time window of about 80% is reached, while the 40 % CF<sub>4</sub> gas mixture permits the triple-GEM to reach more than 90 % efficiency at moderate voltages.

## Contents

<b>1</b>	<b>Introduction</b>	<b>2</b>
<b>2</b>	<b>The triple-GEM detector</b>	<b>2</b>
<b>3</b>	<b>The tests with cosmic rays</b>	<b>2</b>
3.1	The experimental setup	3
3.2	The triple-GEM chamber under test	3
<b>4</b>	<b>Gas simulation with GARFIELD</b>	<b>3</b>
<b>5</b>	<b>Experimental measurements</b>	<b>5</b>
5.1	Measurements with the Ar/CO <sub>2</sub> /CF <sub>4</sub> 40:55:5 mixture	5
5.1.1	Optimization of the detector electric fields	6
5.2	Measurements with the Ar/CO <sub>2</sub> /CF <sub>4</sub> 45:15:40 mixture	7
5.3	Comparison between the two gas mixtures	7
5.4	The pad cluster size	8
<b>6</b>	<b>Conclusion</b>	<b>8</b>
<b>Bibliography</b>		<b>9</b>
<b>7</b>	<b>References</b>	<b>9</b>

## 1 Introduction

The LHCb muon system [1, 2, 3] is composed by 5 rectangular stations (M1-M5) along the beam axis. Each station is divided into 4 regions (R1-R4) equipped with MWPCs. In the central region (R1) of the M1 station, where the particle flux is higher, 12 triple-GEM detectors are used [4]. During the last years of LHCb operation, GEM chambers have shown remarkable rate capability and high aging resistance, and are the natural candidates to constitute the future inner region of the muon system, after the upgrade scheduled in 2018.

So far, the triple-GEM detectors were operated with a gas mixture containing 40% of  $\text{CF}_4$ , different from the one in use for the MWPCs, where this component is 5%. If it will be possible to operate the entire muon detector with a single gas mixture after the upgrade, the gas system will be unique and the costs will therefore be reduced. Testing the triple-GEM efficiency and time resolution with different gaseous mixtures is therefore a significant step in evaluating how to upgrade the muon system when the luminosity in LHCb will reach  $2 \times 10^{33} \text{ cm}^{-2}\text{s}^{-1}$ . For this purpose, a triple-GEM detector was tested with the two gas mixtures currently in use at LHCb: the mixture so far used in the GEM chambers and the one used in the MWPCs.

## 2 The triple-GEM detector

A Gas Electron Multiplier (GEM) is made by a 50  $\mu\text{m}$  kapton foil, clad on each side with a 5  $\mu\text{m}$  copper layer and perforated with a high density of channels. By applying a voltage difference between the copper sides, a high electric field is generated into the holes (Figure 1 left), which act as multiplication channels. A triple-GEM detector consists in three GEM foils sandwiched between an anode and a cathode, as shown on the right of Figure 1, filled with a suitable gas mixture. The primary electrons

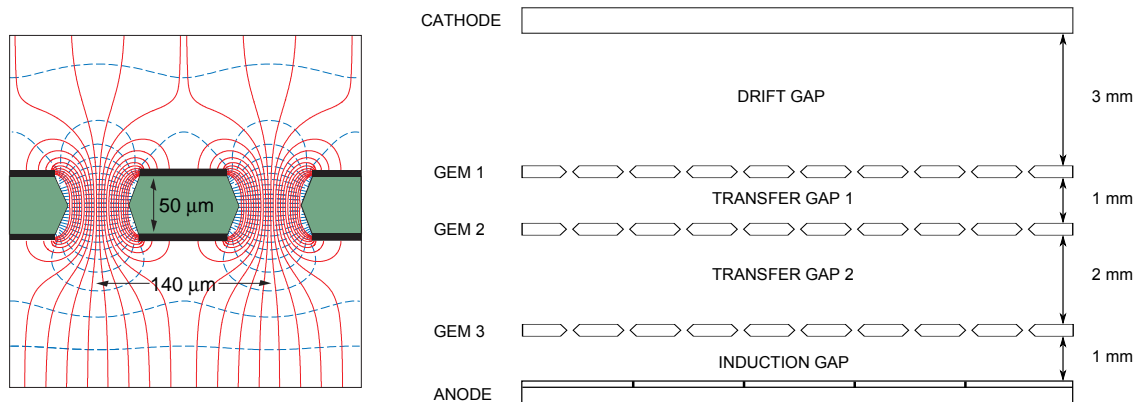


**Figure 1** Left: schematic view and typical dimensions of the hole structure in the GEM amplification cell with electric field lines (solid) and equipotential lines (dashed). Right: cross section of a triple-GEM detector.

generated in the drift gap are multiplicatively multiplied by passing through the three GEM foils, and induce a signal on the anode pads. In this layout, high gain (i.e. high electron multiplication) can be reached with relatively low voltages across the GEM planes, therefore reducing the discharge probability. Suitable choices of the electric fields between the GEM planes permit to operate in a high efficiency region with a fast response, even at the high particle flux encountered in M1R1.

## 3 The tests with cosmic rays

Performance analysis of the triple-GEM detector were conducted with cosmic rays, at the Sapienza University of Rome. Several measurements were taken using two gas mixtures with the following volume percentages:

- Ar/CO<sub>2</sub>/CF<sub>4</sub> 40:55:5 (named **A** gas mixture),
- Ar/CO<sub>2</sub>/CF<sub>4</sub> 45:15:40 (named **B** gas mixture),

so far used in the LHCb MWPCs and GEMs, respectively. The gases are contained in premixed gas bottles.

### 3.1 The experimental setup

The experimental setup is sketched in Figure 2. An aluminum structure houses two 1.5 m long scintil-

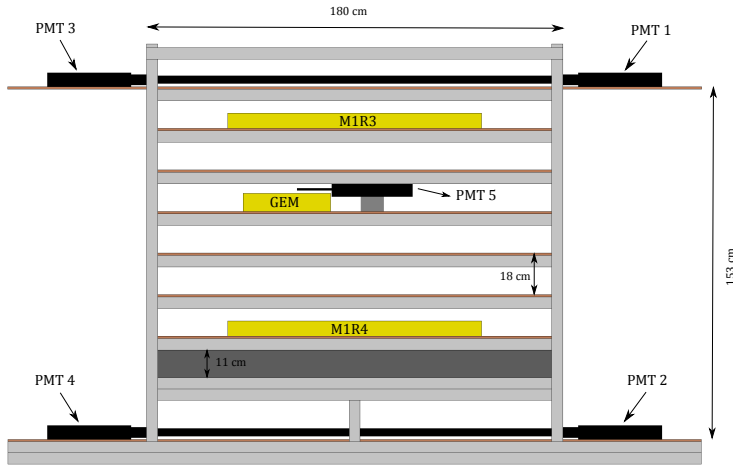


**Figure 2** The experimental setup.

lator paddles and a  $10 \times 10 \text{ cm}^2$  scintillator. The coincidence between these detectors gives the trigger signal to the DAQ. A lead filter was used to select penetrating particles. Two large MWPCs are used to reconstruct the muon direction and to select vertical tracks. For a complete description of the experimental setup, see [8, 9, 10, 11].

### 3.2 The triple-GEM chamber under test

In the LHCb muon system, couples of GEM chamber are logically ORed to ensure the desired detection efficiency. The detector in test is made by only one triple-GEM chamber. The anode plane is segmented in pads following a chessboard texture where each pad is  $1 \times 2.5 \text{ cm}^2$  wide. The signals are read-out and discriminated by means of the CARDIAC-GEM Front-End Board (FEB) [12]. Each FEB manages 8 pads from the tested GEM chamber, for a total of 64 active channels (i.e. 1/3 of the GEM total active surface). Figure 3 shows the instrumented GEM and its acquired area. The FEBs are controlled by mean of a service board using I<sup>2</sup>C protocol. A specifically designed VisualC software permits the setup of the boards (e.g. thresholds setting, channel masking) and the noise rate monitoring.

## 4 Gas simulation with GARFIELD

The main request for the muon chambers at LHCb is a high detection efficiency in the bunch crossing time window (25 ns). Thus, beside to a high overall efficiency, the detectors must ensure a good time performance, which in the GEM chamber is related to the statistics of clusterization in the drift gap. For a minimum ionizing muon traversing the GEM, the number of ionization clusters produced in the drift gap follows a Poissonian distribution, with a mean value that depends on the gas mixture. Therefore, the distance  $x$  of the ionization cluster closer to the first GEM follows the probability distribution  $P(x) = ne^{-nx}$ , with  $\sigma(x) = 1/n$ , and  $n$  being the number of ionization clusters per unit length.

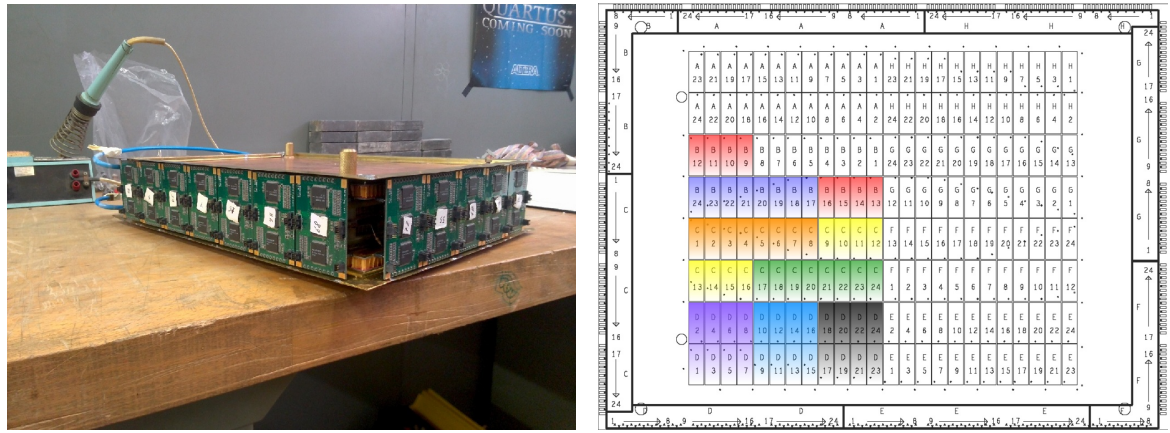


**Figure 3** Photo of the tested GEM chamber. On the right, the acquired pads; each group of 8 pads is read by one FEB.

If the first cluster is always detected, the detector time resolution would be  $\sigma(t) = 1/nv_{drift}$ . Thus, to improve time resolution, a gas mixture with large clusterization and high drift velocity should be used.

The software GARFIELD [5] is employed to perform a simulation of the two gas mixtures involved in the experimental study, focusing on the clusterization ( $n$ ) and the electron drift velocity ( $v_{drift}$ ). To study the specific clusterization caused by a minimum ionizing muon traversing the gas, muons that vertically traverse a 3 mm gap are generated, under a 3 kV/cm electric field. The mean number of clusters produced per track is  $n_A = 46$ , 4 clusters/cm for the 5% CF<sub>4</sub> mixture (Figure 4) and  $n_B = 57$ , 4 for the 40% CF<sub>4</sub> mixture (Figure 5).

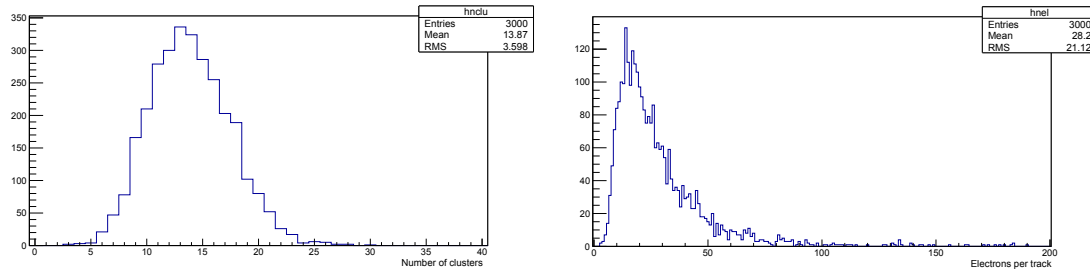


**Figure 4** Distributions of the number of clusters and number of electrons per track in the **A** gas mixture.

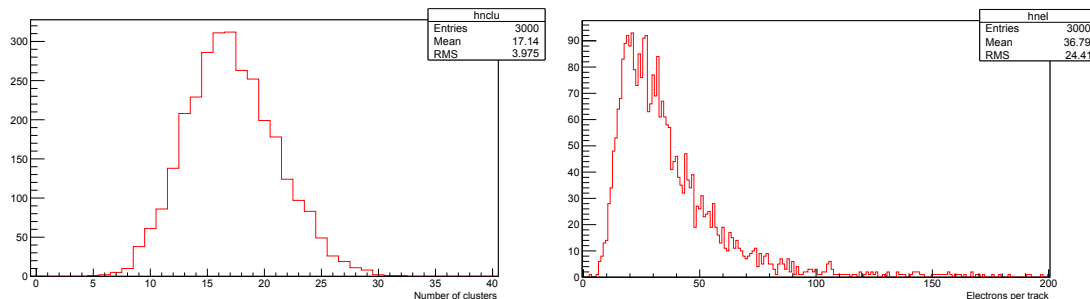


**Figure 5** Distributions of the number of clusters and number of electrons per track in the **B** gas mixture.

Figure 6 (left) shows the simulated electron drift velocity as a function of the electric field: the larger CF<sub>4</sub> component leads to a higher drift velocity, resulting in a faster detector response. By combining the aforementioned results, Figure 6 (right) shows the  $\sigma(t)$  term, representing the statistical contribu-

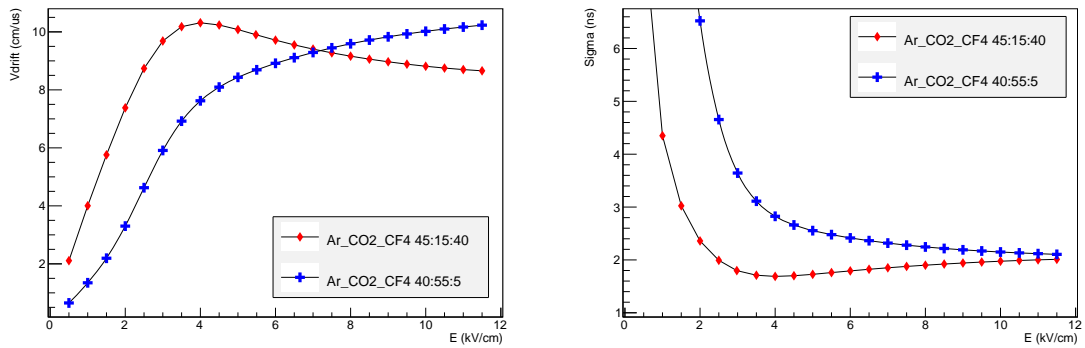


**Figure 6** Simulated drift velocity for the two Ar/CO<sub>2</sub>/CF<sub>4</sub> mixtures. On the right, statistical contribution to the time resolution.

bution to the time resolution. This quantity sets a limit to the time resolution of gap-based gaseous detectors, as previously described. It can be observed that for an electric field value of about 3 – 4 kV/cm, which are typical values for the field in the GEM drift gap, the larger CF<sub>4</sub> percentage in the gas mixture is expected to allow better time performance of the detector.

## 5 Experimental measurements

In order to study the performance of the triple-GEM chamber with the two gas mixtures and to check the results of the simulation, several measurements were taken with cosmic rays. In each data taking run, 20000 events were acquired. The signal arrival times were recorded by a 128 channel TDC and the data were subsequently analysed by using a specific ROOT [6] program.

Figure 7 shows typical time spectra of the triple-GEM chamber: their width is an indicator of the chamber time resolution.

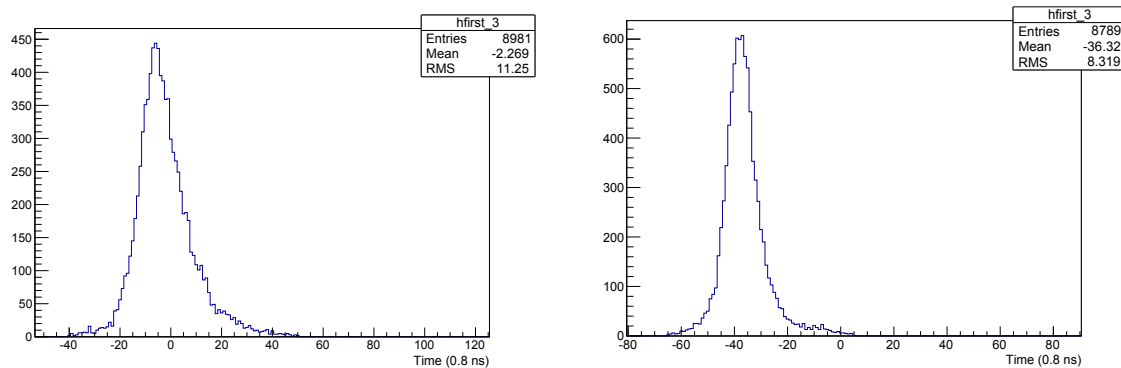


**Figure 7** Response time spectra of the GEM chamber, in the electric configuration  $E_d = 3.0$  kV/cm  $E_{t1} = E_{t2} = 3.0$  kV/cm  $E_i = 5.0$  kV/cm with a total tension of  $V_{gem} = V_{gem1} + V_{gem2} + V_{gem3} = 1315$  V. On the left, the spectrum is measured with the **A** gas mixture, while the right spectrum is obtained with the **B** mixture. The time is measured in TDC registers where 1 reg = 0.8 ns.

### 5.1 Measurements with the Ar/CO<sub>2</sub>/CF<sub>4</sub> 40:55:5 mixture

A first set of measurements was taken by using the **A** gas mixture. The detection efficiency is measured varying the voltage applied to the GEM foils. The increase of the sum of the voltages ( $V_{gem} = V_{gem1} + V_{gem2} + V_{gem3}$ ) leads to a higher signal amplification, i.e. a higher gain. As can be observed in Figure 8 (left), the efficiency settles on a plateau at  $\epsilon \simeq 95\%$  when  $V_{gem} > 1270$  V.

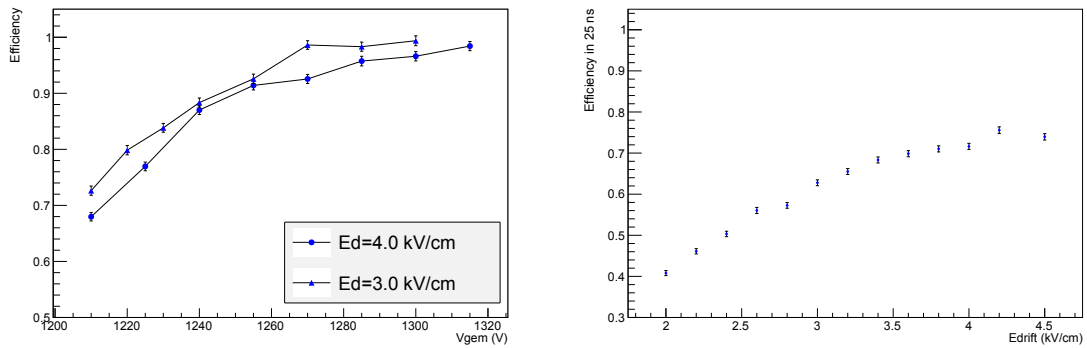


**Figure 8** Left: detection efficiency as a function of the total voltage applied over the 3 GEM foils, for  $E_d = 3$  kV/cm and 4 kV/cm. Right: measured 25 ns efficiency as a function of  $E_d$ , at  $V_{gem} = 1255$  V.

### 5.1.1 Optimization of the detector electric fields

A detailed analysis of the GEM performances is carried out in order to find the optimal values of the chamber electric fields. In this work, the voltage on the GEM foils is kept to an intermediate value of  $V_{gem} = 1255$  V, where the sensitivity to efficiency variations is higher: in a region of saturated efficiency, fluctuations would be barely observable.

**The drift field** In Figure 8 (right), a systematic study on the effect of the drift field value is shown. As one can expect from the GARFIELD simulation, the increase of the drift field from 3.0 to 4.0 kV/cm leads to a faster electron drift, which in turns leads to better detector time performance: the 25 ns efficiency increases, reflecting the trend seen in Figure 6. On the other hand, the detection efficiency is quite unaltered. Note that setting a too high electric field value prevents the field lines in the gap to match up with the GEM field lines, leading to electron defocussing effect and therefore to inefficiency. As a results of this analysis the drift field was set to 4 kV/cm.

**The transfer fields** For values above 2 – 3 kV/cm, transfer fields do not alter the GEM performance in a significant way, as can be seen in Figure 9. We therefore fix  $E_{t1} = E_{t2} = 3.0$  kV/cm  $\equiv E_t$ .

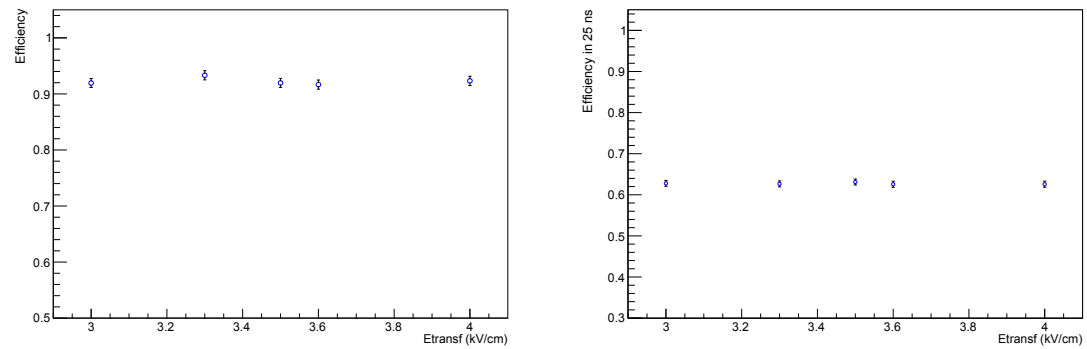


**Figure 9** Left: efficiency as a function of  $E_t$ . Right: 25 ns efficiency as a function of  $E_t$ .

Increasing the field in the transfer gaps causes electron clouds to drift faster: Figure 10 (left) shows the mean time shift caused by higher transfer field values. The behaviour of the response time and the total time anticipation (12.8 ns) are well compatible with the simulated drift velocities and a 3 mm total path for the two transfer gaps. This result therefore confirms that the simulation is able to correctly reproduce the electron drift process within the gas mixture.

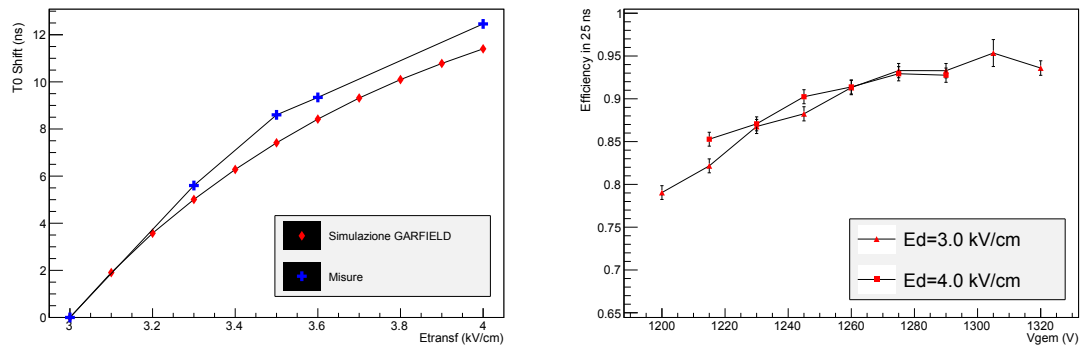


**Figure 10** Left: mean GEM response time shift caused by the transfer field rise. The time value  $T_0 = 0$  is assigned when  $E_t = 3.0 \text{ kV/cm}$ . Right: 25 ns efficiency as a function of the GEM tension, measured with the **B** gas mixture.

## 5.2 Measurements with the Ar/CO<sub>2</sub>/CF<sub>4</sub> 45:15:40 mixture

The tests on efficiency were repeated in the same way for the **B** gas mixture. A little improvement in the detection efficiency is observed and, more importantly, the detection efficiency in 25 ns is found to be significantly higher: values over 90 % are measured at intermediate voltages (Figure 10, right). Rising the drift field from 3 to 4 kV/cm increases the detector time performances slightly, as can be expected from the simulated drift velocity for this gas mixture (Figure 6, left). It is thus possible to

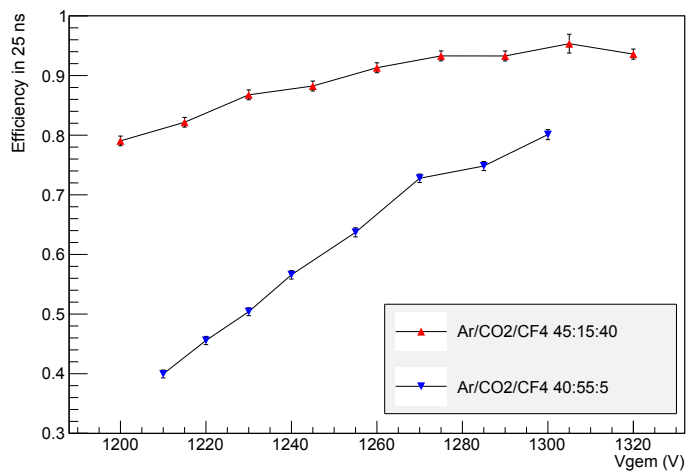


**Figure 11** Measured values of the 25 ns efficiency in the two gas mixtures, with  $E_d = 3.0 \text{ kV/cm}$ .

conclude that the performance measured with this setup for a triple-GEM detector operated with the **B** gas mixture are in very good agreement with the ones found in all previous tests and on the LHCb apparatus [13, 14, 15].

## 5.3 Comparison between the two gas mixtures

The results obtained with the different gas mixture are compared. Figure 11 shows the measured detection efficiency in 25 ns for the two gas mixtures. The advantage of the large CF<sub>4</sub> component in the **B** mixture is clear: the time performances are rather better when the drift velocity and the ionization yield are larger, as anticipated in Section 4.

## 5.4 The pad cluster size

Another fundamental parameter to monitor is the pad cluster size (CS), defined as the number of pads fired in each event within a 25 ns time window. This measurement is performed by only considering the horizontal size of the cluster, crucial for the momentum resolution of the LHCb muon spectrometer. As shown in Figure 12 (left), the cluster size for the **A** gas mixture is always under 1.05, largely below the 1.2 limit required in the experiment for the GEM chambers. Higher cluster size values are observed in the **B** mixture, but still below the 1.2 limit. The observed CS values are also indications of the gain values for the gas mixtures. A larger CS suggests a higher gain for the **B** mixture that can be explained by the larger Ar/CO<sub>2</sub> ratio<sup>a</sup>.

The 25 ns efficiency and cluster size are monotonically increasing functions of the gain, and they only weakly depend on the other gas properties like the specific ionization and the drift velocity. If the latter dependence could be neglected, the dependence of the 25 ns efficiency on the cluster size would be independent of the gas mixture. As shown in Figure 12 (right), the two datasets (**A** and **B**) occupy two separate regions of the  $\epsilon_{25}$  – CS plane. In particular, the **B** mixture has higher performance and higher cluster size, indicating a higher gain. On the other hand, the **A** gas mixture seems to have a lower gain for all voltage values taken into account. The lower gain, along with the lower electron drift velocity and lower clusterization, explain the lower performance provided by the **A** mixture.

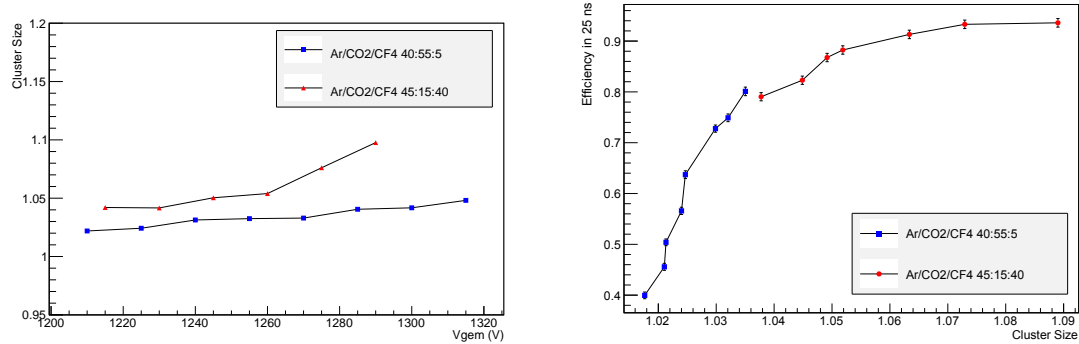


**Figure 12** Left: mean value of the cluster size as a function of the GEM voltage, measured in the two gas mixtures. Right:  $\epsilon_{25}$  vs CS for the two gas mixtures.

## 6 Conclusion

With the incoming LHCb upgrade in 2018, the triple-GEM chamber performances have been investigated with two different gas mixtures, so far used in the LHCb MWPCs (Ar/CO<sub>2</sub>/CF<sub>4</sub> 40:55:5) and GEM detectors (Ar/CO<sub>2</sub>/CF<sub>4</sub> 45:15:40).

After several studies of electric fields optimization, measurements of detection efficiency and cluster size were performed by varying the voltage applied to the GEM foils. As predicted by the GARFIELD simulation, the results confirmed a drop of the GEM time performances if the CF<sub>4</sub> component in the mixture decrease from 40% to 5%. At the same time, cluster size results suggest a lower gain for the 5% CF<sub>4</sub> mixture.

The results from the present work provide useful functional GEM parameters for an evaluation, through an extended Monte Carlo simulation, of the global performances of the 2018 LHCb muon system.

<sup>a</sup>For a description of the Ar/CO<sub>2</sub>/CF<sub>4</sub> properties in a gaseous detector, consult [7].

## 7 References

- [1] LHCb Collaboration, *Muon System TDR*, CERN/LHCC/2001-010 (2001)
- [2] LHCb Collaboration, *Addendum to the Muon System TDR*, CERN/LHCC/2003-002 (2003)
- [3] LHCb Collaboration, *Second Addendum to the Muon System TDR*, CERN/LHCC/2005-012 (2005)
- [4] LHCb Collaboration, *The LHCb Detector at the LHC*, 2008 JINST 3 S08005 (2008)
- [5] R. Veenhof, *Garfield - simulation of gaseous detectors*, <http://garfield.web.cern.ch/garfield/>
- [6] Rene Brun and Fons Rademakers, *ROOT - An Object Oriented Data Analysis Framework*, Proceedings AIHENP'96 Workshop, Lausanne, Sep. 1996, Nucl. Inst. & Meth. in Phys. Res. A 389 (1997) 81-86.
- [7] F. Sauli, *Principle of operation of multiwire proportional and drift chambers*, CERN 77-09 (1977)
- [8] M. Santimaria, *Studio del rivelatore GEM per l'upgrade dell'esperimento LHCb*, CERN-THESIS-2013-296
- [9] R. Antunes Nobrega, V. Bocci, E. Furfaro, G. Martellotti, G. Penso and D. Pinci, *Performance of the MWPC of the first station of the LHCb Muon System*, IEEE Nucl. Sci. Symp. Conf. Rec. (2009) 797.
- [10] G. Martellotti, R. Nobrega, E. Fufaro, G. Penso and D. Pinci, *Study of the performance of the LHCb MWPC with cosmic rays*, CERN-LHCB-2008-057.
- [11] E. Furfaro, G. Martellotti, R. Nobrega, G. Penso and D. Pinci, *Study of the performance of the LHCb muon chambers with cosmic rays*, JINST 6 (2011) P12002
- [12] S. Cadeddu et al. *The DIALOG chip in the front-end electronics of the LHCb muon detector*, IEEE Trans. Nucl. Sci. 52 (2005) 2726.
- [13] G. Bencivenni et al., *A triple GEM detector with pad readout for high rate charged particle triggering*, Nucl. Instrum. Meth. A 488 (2002) 493.
- [14] G. Bencivenni et al., *A fast multi-GEM-based detector for high-rate charged-particle triggering*, IEEE Trans. Nucl. Sci. 49 (2002) 3242.
- [15] D. Pinci, *A triple-GEM detector for the muon system of the LHCb experiment*, CERN-THESIS-2006-070.
- [16] J. Beringer et al. (Particle Data Group), Phys. Rev. D86 Sec. 31, 010001 (2012)